



# Range, energy loss, energy straggling and damage production for $\alpha$ -particles in uranium dioxide

Hj. Matzke \*

*European Commission, Joint Research Centre, Institute for Transuranium Elements, P.O. Box 2340, D-76125 Karlsruhe, Germany*

Received 11 May 1998; accepted 22 July 1998

## Abstract

Energy loss and energy straggling of  $\alpha$ -particles in  $\text{UO}_2$  were measured for  $\alpha$ -energies up to 8.78 MeV.  $\alpha$ -sources of Pu-239 and a 'multi-energy source' emitting  $\alpha$ -particles of five different energies obtained by recoil implantation from a Th-228 source were coated with  $\text{UO}_2$  layers of 17 different thicknesses. Confirmation of these results was obtained from Rutherford backscattering spectroscopy, RBS/channeling experiments with  $\text{UO}_2$  single crystals preimplanted with He-ions. The measured energy loss values were used to deduce the range-energy relation. The results are in good agreement with calculations using the code TRIM 96. The energy straggling results are discussed in the frame of Bohr's theory. Finally, defects and damage produced by  $\alpha$ -particles and He-ions in  $\text{UO}_2$  are briefly treated. © 1999 Elsevier Science B.V. All rights reserved.

## 1. Introduction

In recent years, the slowing down of  $\alpha$ -particles has been increasingly used to study solid state properties of nonmetals; in particular,  $\alpha$ -particles and He-ions have been used to investigate interesting properties of nuclear ceramics, such as  $\text{UO}_2$ . The decrease in energy of (mono-energetic)  $\alpha$ -particles after passing through a solid can be used to determine diffusion profiles of  $\alpha$ -emitting tracers, such as U-233 in  $\text{UO}_2$  [1,2]. Surface properties, crystal perfection and radiation damage can be measured employing Rutherford backscattering spectroscopy, RBS, of He-ions combined with the channeling technique [3,4]. To evaluate the data, information on range and energy loss must be available and the energy straggling should be known as well. Energy straggling places a finite limit for which energy losses, and hence depths can be resolved, and it impairs the ability to identify masses by RBS, except for atoms located at the surface. Energy loss (stopping power) measurements have been published in the 1960/1970s for many materials including the nuclear ceramics UC,  $\text{UO}_2$  and  $\text{ThO}_2$

[5–8]. In contrast, energy straggling has usually only been measured for metals and for some gaseous absorbers.

In the present paper, range and straggling values for today's fuel used in electricity producing nuclear power stations, i.e. uranium dioxide, are reported, analysed and compared with calculations performed with the computer code TRIM 96 [9]. Energy loss values are also briefly treated.

## 2. Experimental

Thin mono-energetic sources of Pu-239 ( $E_\alpha = 5.16$  MeV) produced by flash evaporation or multienergy sources, i.e. platelets exposed to a recoil source of Th-228, were used. The platelets exposed to Th-228 contained the daughter products of Th-228, i.e. Ra-224 (5.68 MeV), Rn-220 (6.29 MeV), Po-216 (6.78 MeV), Bi-212 (6.05 MeV with 30%  $\alpha$ -emission), and Po-212 (8.78 MeV). In this way, different energies up to 8.78 MeV could be used with one  $\alpha$ -source. The sources were successively coated with  $\text{UO}_2$  layers using a small electron beam furnace. The layer thicknesses were determined by weighing. They varied between 0.16 and 1.6  $\mu\text{m}$  (accuracy  $\sim 2.5\%$ ). A total of 17 layers were pro-

\* Tel.: +49-7247 951 273; fax: +49-7247 951 590.

duced leading to a maximum total thickness of 11  $\mu\text{m}$ . The layers were crystalline with the fluorite structure. X-ray diffraction confirmed that the deposited  $\text{UO}_2$  was nearly stoichiometric. RBS analysis was used to detect possible impurities. No impurities were found. Energy loss and energy straggling were measured with conventional surface barrier Si-detectors. The resolution of the detectors for 5 MeV  $\alpha$ -particles was about 18 keV (full width at half maximum (FWHM),  $\eta_d$ ). The error in energy measurements was  $<1\%$ .

For application and confirmation of these data,  $\text{UO}_2$  single crystals were implanted with 1 MeV  $\text{He}^+$ -ions with different fluences up to  $1.1 \times 10^{17}$  ions/ $\text{cm}^2$ . These crystals were analyzed by RBS/channeling at the Dynamitron Tandem Laboratory at the Ruhr Universität Bochum (Dr M. Wielunski). Analysis was done at different energies: 3.5, 4.5, 6, 7.5 and 9 MeV in both random and aligned mode. For the high energies, resonance scattering  $\text{O}^{16}(\alpha, \alpha)\text{O}^{16}$  occurred, giving rise to a significant increase in the scattering yield for the oxygen sublattice (see Section 4).

### 3. Theoretical

The theory of particle–solid interactions and of stopping of ions in matter dates back to the early days of the century and comprises the work of famous physicists such as Bohr, Bethe, Bloch and others [10,11]. There is also a good description of the physics involved in the book of Olander [12] and tables for ranges and stopping powers exist for many elements (e.g. Ref. [13]). For the energy loss, the Bethe–Bloch formula [10] is still often used

$$-\frac{dE}{dx} = \frac{4\pi z^2 e^4}{mv} \frac{NZ}{A} \left( \ln \frac{2mv^2}{I} - \frac{C}{Z} \right). \quad (1)$$

Here,  $e$  and  $m$  are the electron charge and mass,  $v$  and  $z$  are the velocity and charge ( $z=2$ ) of the  $\alpha$ -particle,  $N$  is Avogadro's number,  $A$  and  $Z$  are the atomic weight and number of the target material, and  $I$  is the mean excitation potential.  $C/Z$  are shell corrections allowing for the case that for lower energies the velocity of the  $\alpha$ -particle is no longer large compared with the velocity of the inner electrons in their orbitals. In Eq. (1), terms that can be neglected have been omitted (essentially terms related to relativity and density corrections). For a compound like  $\text{UO}_2$ ,  $dE/dx$  is calculated separately for U and O, and multiplying the results with weight factors  $W_n = A_n/(A_O + A_U)$  ( $n = \text{O or U}$ ).

There are, of course, a number of other and more recent approaches to theoretically predict  $dE/dx$  values. Since emphasis of this short paper is on experimental work to determine ranges and straggling, this literature is not discussed. Comparison is, however, made with

TRIM calculations. Also the present experimental results, when compared with Eq. (1) are tentatively used to deduce information on the shell correction term  $C/Z$ .

Statistical fluctuations in the number and kind of collisions along the tracks of  $\alpha$ -particles cause unequal energy losses for different particles starting under identical conditions. The theoretical understanding of this range or energy straggling is well advanced and different treatments are available, e.g. Refs. [11,14–16] and others.

Gaussian distributions are expected for energy losses of a few percent up to about 70% [17]. Asymmetry and even decreased straggling (beyond the maximum of the energy loss) can occur at larger energy losses [18,19].

The simplest of the available straggling expressions is owing to Bohr [11]. This expression is used as example though, as for energy loss, other theories exist as well. The standard deviation of the Gaussian distribution is given as

$$\Omega_s^2 = 4\pi z^2 e^4 NZ (\Delta\xi), \quad (2)$$

where  $ze$  is the charge of the ion passing through the layer  $\Delta\xi$  of a material of atomic number  $Z$  containing  $N$  atoms per  $\text{cm}^3$ . Often, the denomination  $\Omega_B$  is used in the literature ( $s$  stands for straggling,  $B$  for Bohr). Note that the FWHM  $\eta = 2(2 \ln 2)^{1/2} \Omega_s = 2.35 \Omega_s$  and that the width due to straggling will add quadratically to the width due to the limited resolution of the detector,  $\eta_d$ . Hence

$$\eta^2 = (\eta_{\text{total}})^2 - \eta_d^2. \quad (3)$$

According to Bohr's theory, a plot of the standard deviation of straggling,  $\Omega_s$ , versus the square root of depth or layer thickness,  $\sqrt{\Delta\xi}$ , should be a straight line. (Equally, the other conventional means of presenting straggling results, i.e. a plot of  $\Omega_s^2$  versus  $\Delta\xi$  should also be a straight line) Furthermore, energy straggling should be independent of the incident energy of the  $\alpha$ -particles.

Most reported experimental results have been obtained for metals. They are often not very well represented by any of the theories, particularly at low energies, though sometimes reasonable agreement is observed for high energies and small thicknesses. The experimental values can be both larger and smaller than Bohr's predictions (e.g. Refs. [18,19]).

Calculations of ranges and straggling were also performed with the TRIM-code, version TRIM 96 [9]. When applicable, displacement energies  $E_d$  for U of 40 eV and for O of 20 eV were used.

### 4. Results and discussion

Fig. 1 shows  $\alpha$ -spectra of the multienergy source before and after evaporating  $\text{UO}_2$  layers with a total

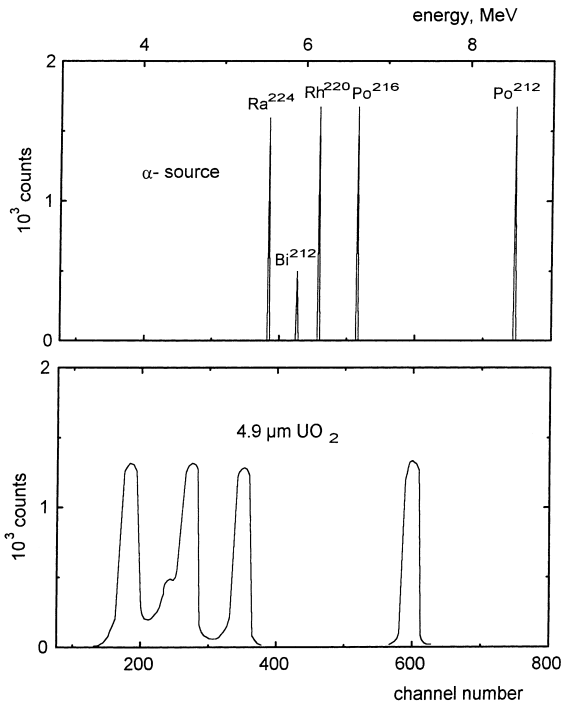


Fig. 1. The  $\alpha$ -energy spectra of a multienergy source before and after coating with 4.9  $\mu\text{m}$   $\text{UO}_2$ .

thickness of 4.9  $\mu\text{m}$  onto the source. As expected, the line spectra of the 5  $\alpha$ -emitters after coating with  $\text{UO}_2$  layers. For the 17 layers produced, energy loss and energy straggling values could be obtained (for five different  $\alpha$ -energies). For all thicknesses at least some of the  $\alpha$ -lines could still be separated. The results obtained are shown in Fig. 2. As expected, the low intensity line of Bi-212 with  $E_x = 6.05$  MeV could only be used at small thicknesses. These curves can be joined together, as also shown in Fig. 2. An arrow indicates the procedure for the case of Po-216 (6.78 MeV). The resulting curve represents thus the energy loss of  $\alpha$ -particles of 8.78 MeV original energy in  $\text{UO}_2$  layers of up to 22  $\mu\text{m}$  thickness.

A simple algorithm was deduced from all these measurements to describe the energy loss values in the form  $dE/dx = 1/(AE + B)$  where the constants  $A$  and  $B$  are given in Eq. (4). Additional supporting results of the same type were obtained with the mono-energetic source of Pu-239.

$$\frac{dE}{dx} = \frac{1}{0.358E + 1.20} \text{MeV}/\mu\text{m} \quad (\text{for } E \geq 1 \text{ MeV}). \quad (4)$$

The relation between the depth  $x$  of the  $\alpha$ -emitting atom beneath the surface (or between the thickness of

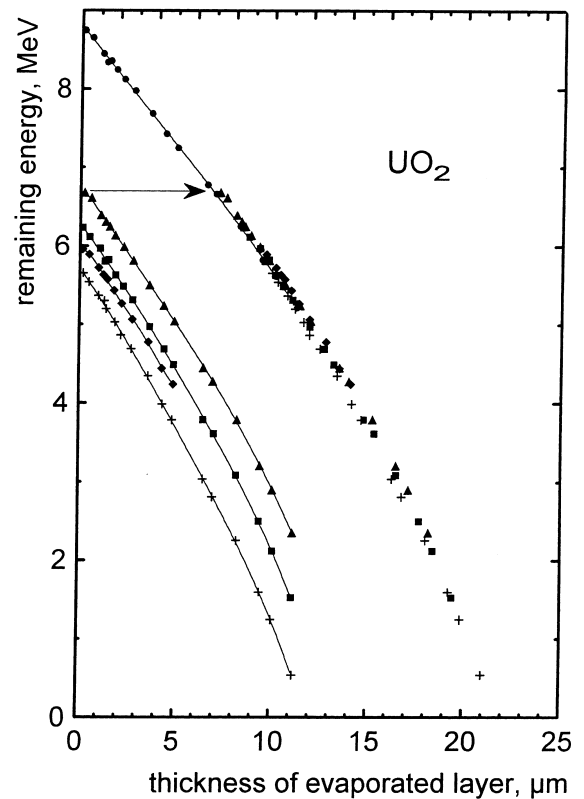


Fig. 2. Remaining  $\alpha$ -peak energy of the five  $\alpha$ -emitters of the multienergy source after having passed different thicknesses of  $\text{UO}_2$ . A composite curve is constructed by joining the curves for the five  $\alpha$ -energies into one curve (see arrow: data points not joined by a full line).

the absorbing  $\text{UO}_2$  layer), the initial energy  $E_0$  (decay energy) and the remaining energy  $E$  can be obtained by integration of Eq. (4) yielding

$$x = 0.179(E_0^2 - E) + 1.20(E_0 - E) \quad (5)$$

giving the range as a function of initial energy  $E_0$  by setting  $E=0$ . The resulting ranges are shown in Fig. 3, where they are compared with TRIM calculations. Agreement is seen to be rather good. The experimental values are, however, consistently lower by 0.5–1  $\mu\text{m}$  than the calculated values. The relative difference is largest for low energies, i.e. for those used for normal RBS analysis.

There are several reasons for discrepancies at low energies: (i) the shell correction term becomes important at low energies (see below), and it is not well known, (ii) the curve of  $dE/dX$  versus  $E$  shows a maximum at low energies and (iii) the He-ions have an effective charge of  $<2$  at low energies. As examples, for He-ions in U-metal, the maximum in  $dE/dX$  occurs at 0.9 MeV and  $dE/dX$  decreases by a factor of 2 at 0.13 MeV [13] and He-ions

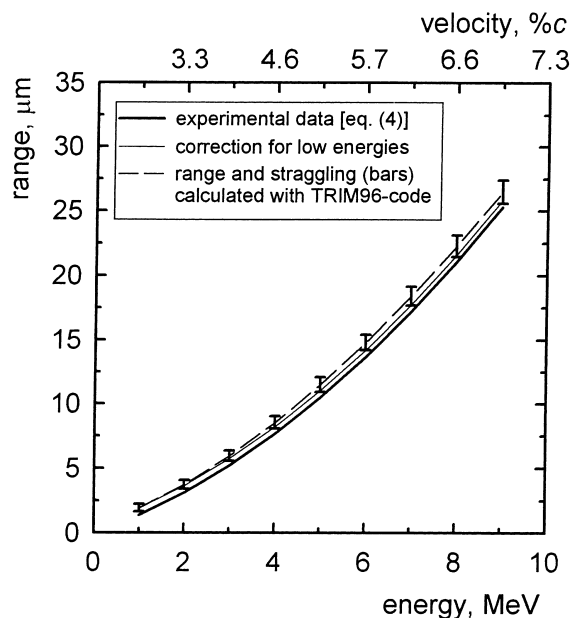


Fig. 3. Range-energy relation of  $\alpha$ -particles in  $\text{UO}_2$ . Comparison of the experimental results with calculations with the code TRIM 96. TRIM results for range straggling are included.

reach the effective charge of 2+ only at  $\sim 0.5$  MeV energy. An effective charge between 1 and 2 leads also to lower energy loss values (see e.g. Eq. (1)). If the energy dependence of  $dE/dX$  of He in U-metal for  $E < 1$  MeV [13] is used to estimate the effect on the range values of Fig. 3 for  $\text{UO}_2$ , an increase in the range by  $0.52 \mu\text{m}$  is obtained. This is in excellent agreement with the TRIM calculation for  $E = 1$  MeV, although the data according to Eq. (4) remain slightly lower than the TRIM calculations for higher energies.

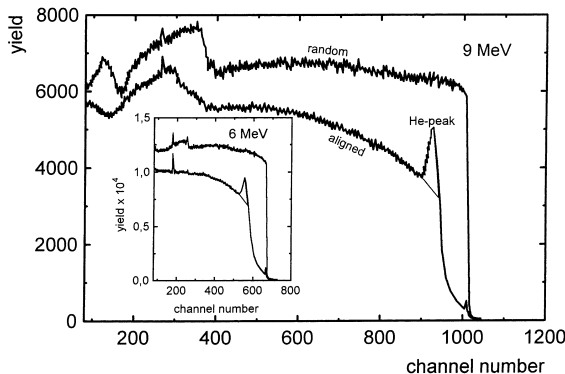


Fig. 4. Rutherford backscattering and resonance scattering spectra of 9 MeV He-ions from a  $\text{UO}_2$  single crystal implanted at room temperature with 1 MeV He-ions to a total fluence of  $1.1 \times 10^{17}$  ions/cm<sup>2</sup>. The inset shows the spectra for 6 MeV He-ions.

Fig. 4 shows two of the RBS/channeling spectra or resonance scattering/channeling spectra for a  $\text{UO}_2$  single crystal preimplanted with 1 MeV He-ions and analysed with high energy He-ions. The spectra for 9 and 6 MeV are shown. Additional runs were made for 7.57, 4.5 and 3.5 MeV energy of the analyzing beam. The three peaks for resonance scattering (e.g., Refs. [20–22]), corresponding to three large maxima of the scattering cross-section for  $\text{O}^{16}(\alpha, \alpha)\text{O}^{16}$  resonance scattering, located between 7.4 and 7.6 MeV and around 7.2 and 7.0 MeV, were most clearly observed for 7.57 MeV He-ions. Because a larger He-ion energy for analysis was used than for implantation, the backscattering investigation allows the detection of the damage produced by He, in principle separately in the oxygen and in the uranium sublattices. As expected, most damage is formed at the end of the range of the He-ions, as evidenced by the peaks for U-defects in the aligned spectra labelled He-peak in Fig. 4. Such He-damage peaks were observed for all energies of the analyzing He-beam. TRIM calculations and the existing experimental experience on many materials show that damage peaks are only slightly displaced (to a slightly smaller depth) from the range peaks of the implanted ions. The backscattering spectra yield therefore additional confirming data on energy loss for the five energies used for the analyzing beam, in good agreement with the results of Eq. (4) and Fig. 3. For instance, the mean depth of the He-damage peak was  $1.34 \mu\text{m}$ , as compared to  $1.38 \mu\text{m}$  for the range as obtained from Eq. (4). Note, however, that the above-mentioned corrections upwards towards  $1.86 \mu\text{m}$  for the range 1 of MeV He-ions should be made. The corresponding numbers of TRIM 96 calculations are 1.95 and  $2 \mu\text{m}$ .

From the size of the He damage peaks and the known fluence of the 1 MeV He-ions, the number of permanently displaced U-atoms per implanted He-ion can be deduced to be 3. Approximately 60 U-defects are expected to be formed per He-ion. Most defects are, therefore, recovered. Instantaneous defect recovery in  $\text{UO}_2$  has been previously measured following implantation with heavy ions (Kr, Te and Cs) of 40 keV energy [23]. For high fluences, instantaneous recovery was even more pronounced in the dense collision cascades produced by these heavy ions of lower energy: At a fluence of  $5 \times 10^{16}$  ions/cm<sup>2</sup>, for example, less than 1 U-defect per incoming ion survived of the  $\sim 250$  defects expected to have been formed. This effective defect recovery is a main reason for the known radiation stability of  $\text{UO}_2$ . All measured  $\alpha$ -peaks for layer thicknesses,  $\Delta\zeta$ , up to  $5 \mu\text{m}$  were well described by Gaussians distributions. For larger thicknesses, overlapping of some  $\alpha$ -peaks of the multienergy source occurred. A plot of  $\Omega_s^2$  versus  $\Delta\zeta$  could be fitted to a straight line (with  $\Omega_s$  in MeV and  $\Delta\zeta$  in  $\mu\text{m}$ ) without showing any obvious dependence on incident energy as shown in Fig. 5

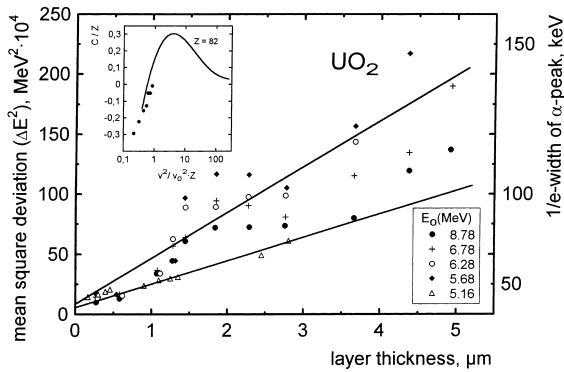


Fig. 5. Measured energy straggling as a function of layer thickness for different incident  $\alpha$ -energies. The inset shows a possible dependence of the shell corrections on particle velocity.

$$\Omega_s^2 = (33 \pm 7) \times 10^{-4} \Delta\xi + (3 \pm 1) \times 10^{-4}. \quad (6)$$

Consequently, the data scatter around a horizontal line as predicted by Bohr's theory if plotted as  $\Omega_s/(\Delta\xi)^{1/2}$  versus incident energy (see Fig. 6). The data for 5.16 MeV are low and represent the separate experiments with the mono-energetic Pu-239 source. The remaining data are due to the multienergy sources and were thus obtained with identical  $\text{UO}_2$  layers. There is a definite trend between thin and thick layers, the thin layers yielding a relatively less pronounced straggling than the thicker ones. Except for this observation, no obvious dependence on layer thickness (or remaining particle energy) was observed. The full line corresponds to about 45% of the value predicted according to Bohr's theory. Two thirds of the experimental points lie within the band indicated by the two dashed lines which correspond to 35% and 50% of the Bohr value, respectively. A direct comparison of the TRIM calculations (Fig. 3) with the present results is not possible since the TRIM

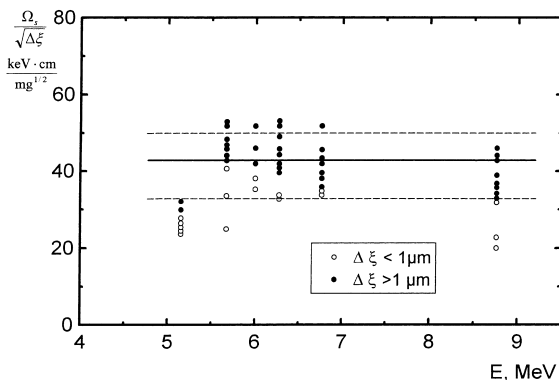


Fig. 6. Measured energy straggling as a function of incident  $\alpha$ -energy.

calculations yielded the range of He-ions in a thick  $\text{UO}_2$  target, whereas experimentally the straggling of  $\alpha$ -particles that passed through thin  $\text{UO}_2$  layers was measured.

As mentioned in Section 2, shell correction terms,  $C/Z$ , are included in Eq. (1). Using available data for Pb on the energy dependence of  $C$  [24], corrections can be made to the calculated energy loss values for low energies. On the other hand, by comparing theory without shell corrections with the experimental data,  $C$ -values for U can be deduced. These (tentative) values are plotted in Fig. 5 as an inset (open circles), and are compared with known values for Pb.

## 5. Summary

In summary, the measured range data of  $\alpha$ -particles in the nuclear fuel  $\text{UO}_2$  are in good agreement with calculations with the TRIM 96 code. The experimental straggling data can be reasonably well fitted to the simple Eq. (6). The trend of the straggling data is not incompatible with the theory of Bohr, although the actual experimental data are only about half as large as the predicted values. Finally, most U-defects formed by the interaction of the He-ions with the  $\text{UO}_2$  are shown to be instantaneously recovered. Similar effective instantaneous defect recovery occurs in the collision cascade of heavy ions of keV energy and is also expected to occur in cascades formed by the recoil daughter atoms of the  $\alpha$ -decay (e.g. 72 keV Th-atoms in the decay of U-238). This is a main reason for the known radiation stability of  $\text{UO}_2$ .

## Acknowledgements

Thanks are due to T. Wiss for performing the TRIM calculations, and to M. Wielunski for the channeling measurements at high He-ion energies.

## References

- [1] A. Höh, Hj. Matzke, Nucl. Instrum. and Meth. 114 (1974) 459.
- [2] Hj. Matzke, Adv. Ceram. 23 (1987) 617.
- [3] Hj. Matzke, A. Tuross, G. Linker, Nucl. Instrum. and Meth. B 91 (1994) 294.
- [4] Hj. Matzke, J. Nucl. Mater. 238 (1997) 58.
- [5] H.J. Hirsch, Hj. Matzke, J. Nucl. Mater. 45 (1972/1973) 29.
- [6] V. Nitzki, Hj. Matzke, Phys. Rev. B 8 (1973) 1894.
- [7] J.F. Marin, M. Coniglio, Nucl. Instrum. and Meth. 42 (1966) 302.
- [8] S. Nasu, K. Ozawa, K. Shiozawa, K. Kawatsura, T. Kurasawa, K. Uchida, J. Nucl. Mater. 73 (1978) 213.

- [9] J.F. Ziegler, J.P. Biersack, U. Littmark, *The Stopping Power and Range of Ions in Solids*, Pergamon, London, 1985 (The TRIM version of 1996, TRIM 96 was used for the present calculations).
- [10] H.A. Bethe, *Ann. Phys. (Leipzig)* 5 (1930) 352; F. Bloch, *Z. Phys.* 81 (1933) 363.
- [11] N. Bohr, *Philos. Mag.* 30 (1915) 581.
- [12] D.R. Olander, *Fundamental Aspects of Nuclear Reactor Fuel Elements*, ch. 17, Techn. Information Center, US Dep. Commerce, Springfield, Virginia, TID-26711-P1, 1976.
- [13] L.C. Northcliffe, R.F. Schilling, *Nuclear Data Tables A* 7 (1970) 233.
- [14] M.S. Livingston, H. Bethe, *Rev. Mod. Phys.* 9 (1937) 245.
- [15] S. Titeica, *Bull. Soc. Rouma. Phys.* 38 (1939) 81.
- [16] J. Lindhard, M. Scharff, *Kgl. Danske Videnskab. Selskab. Mat. Fys. Medd.* 27 (15) (1953).
- [17] C. Tschalär, *Nucl. Instrum. and Meth.* 61 (1968) 141.
- [18] D.S. Sykes, S.J. Harris, *Nucl. Instrum. and Meth.* 94 (1971) 39.
- [19] J.R. Comfort, J.F. Decker, E.T. Lynk, M.O. Scully, A.R. Quinton, *Phys. Rev.* 150 (1966) 249.
- [20] A. Turos, R. Falcone, A. Drigo, A. Sambo, Hj. Matzke, *Nucl. Instrum. and Meth. B* 115 (1996) 359.
- [21] Hj. Matzke, *J. Nucl. Mater.* 238 (1997) 44.
- [22] M. Wielunski, Hj. Matzke, to be published.
- [23] Hj. Matzke, *Nucl. Instrum. and Meth. B* 65 (1992) 30.
- [24] U. Fano, *Ann. Rev. Nucl. Sci.* 13 (1963) 1.